Received: 23 January 2018 | Accepted: 10 May 2018

DOI: 10.1002/jcp.26853

ORIGINAL RESEARCH ARTICLE

WILEY Journal of Cellular Physiology

Establishment of an in vitro organoid model of dermal papilla of human hair follicle

Abhishak C. Gupta[1] | Shikha Chawla[1] | Ashok Hegde[2] | Divya Singh[1] | Balaji Bandyopadhyay[2] | Chandrasekharan C. Lakshmanan[2] | Gurpreet Kalsi[2] | Sourabh Ghosh[1]

[1]Department of Textile Technology, Regenerative Engineering Laboratory, Indian Institute of Technology, Delhi, India

[2]ITC Life Sciences and Technology Centre, ITC Ltd., Bangalore, India

Correspondence
Sourabh Ghosh, Department of Textile Technology, Regenerative Engineering Laboratory, Indian Institute of Technology, Delhi 110016, India.
Email: sghosh08@textile.iitd.ac.in

Funding information
ITC Ltd., India

Human hair dermal papilla (DP) cells are specialized mesenchymal cells that play a pivotal role in hair regeneration and hair cycle activation. The current study aimed to first develop three-dimensional (3D) DP spheroids (DPS) with or without a silk–gelatin (SG) microenvironment, which showed enhanced DP-specific gene expression, resulting in enhanced extracellular matrix (ECM) production compared with a monolayer culture. We tested the feasibility of using this DPS model for drug screening by using minoxidil, which is a standard drug for androgenic alopecia. Minoxidil-treated DPS showed enhanced expression of growth factors and ECM proteins. Further, an attempt has been made to establish an in vitro 3D organoid model consisting of DPS encapsulated by SG hydrogel and hair follicle (HF) keratinocytes and stem cells. This HF organoid model showed the importance of structural features, cell–cell interaction, and hypoxia akin to in vivo HF. The study helped to elucidate the molecular mechanisms to stimulate cell proliferation, cell viability, and elevated expression of HF markers as well as epithelial–mesenchymal crosstalks, demonstrating high relevance to human HF biology. This simple in vitro DP organoid model system has the potential to provide significant insights into the underlying mechanisms of HF morphogenesis, distinct molecular signals relevant to different stages of the hair cycle, and hence can be used for controlled evaluation of the efficacy of new drug molecules.

KEYWORDS
hair follicle, in vitro model, organold

1 | INTRODUCTION

Despite an armamentarium of therapeutic strategies to prevent or reverse hair growth disorders (alopecia, anagen, or telogen effluvium) success is still eluding. There are various causes of alopecia, such as abnormal growth cycle of hair follicle (HF), that is, shortened anagen phase, or reduction in the size of HFs. A few Food and Drug Administration–approved drugs are commonly used to resolve hair loss, for example, oral medicines finasteride, dutasteride, or topically applicable minoxidil. However, these treatments are not yet satisfying because of the side effects, the long duration of therapy and relapses. Minoxidil is reported to cause dermal irritation and unwanted hair growth (Rossi et al., 2012), whereas the use of finasteride has been linked to infertility and psychological problems (Irwig, 2012). Localized inhibition of the JAK–STAT pathway in HF cells by tofacitinib (a medicine for rheumatoid arthritis) or ruxolitinib (a medicine for myeloproliferative diseases) resulted in the rapid onset of hair growth in a mice model (Harel et al., 2015), but their potential for HF regeneration in human is unknown. The search for more efficient drugs is severely slowed down due to the lack of an

anatomically relevant, relatively simpler, well-defined human cell–based three-dimensional (3D) in vitro model of HF.

The HF bulb is a complex organ divided into several components, namely, dermal papilla (DP, a dermal condensate enveloped by epithelial matrix cells and epithelial stem cells), hair matrix, outer and inner root sheath, hair shaft containing terminally differentiated keratinocytes, and connective tissue sheath (Driskell, Clavel, Rendl, & Watt, 2011). During the progression of the hair cycle, DP plays a pivotal role in HF morphogenesis by secreting important regulatory factors that induce the proliferation and differentiation of the epithelial stem cells. Further, epithelial–mesenchymal crosstalks are also crucial for the growth and development of HF (Epstein, Paus, Cotsarelis, & Cotsarelis, 1999). Moreover, the epithelial stem cells express several transcription factors, such as SRY-box9, transcription factor 3 and 4, LIM homeobox 2, and nuclear factor of activated T-cells, which are essential for HF morphogenesis (Blanpain & Fuchs, 2009). These stem cells migrate and provide an extracellular matrix (ECM)–rich micro-environment with a number of regulatory effects to control the signaling dynamics at different stages of the hair development cycle (anagen–telogen–catagen transition; Hsu, Pasolli, & Fuchs, 2011). For example, stem cell niches express high levels of noggin (NOG) and thus help to inhibit bone morphogenic protein (BMP) signaling. Simultaneous upregulation of canonical Wnt–β-catenin signaling is essential for the HF growth (Jahoda & Christiano, 2011; Tiede et al., 2007). Keratinocytes have also been reported to strongly affect HF regeneration, as evidenced by expression of the Col17a1 gene specifically in HF keratinocytes to preserve the quiescence state of the bulge stem cells (Tanimura et al., 2011).

Attempts have been made to develop in vitro and in vivo HF models to investigate the cell–cell and cell–matrix interaction to elucidate the genomics and biochemical dynamics during HF development. HF reconstruction strategies have been reported earlier in a number of rodent models. For example, a coculture model of primary mouse keratinocytes and HF progenitor cells after implantation into nude mice showed a broad differentiation potential of the cultured cells giving rise to distinct parts of the HF (Kamimura, Lee, Baden, Brissette, & Paolo Dotto, 1997). Weinberg et al. reported HF formation on the back of athymic nude mouse using cells from newborn and perinatal mice (Weinberg et al., 1993). The results from this study indicated that the DP cells maintained their follicle inductive property up to 14 passages and contributed to the reconstituted skin (Weinberg et al., 1993). Adult rodent DP, isolated from the HF bulb transplanted into recipient skin, could induce de novo HF neogenesis and hair development (Ohyama et al., 2006). These models provided essential insights into the in vivo HF regeneration upon implantation of a mixed HF cell population. However, since most of these studies used rodent cell–based assays, their relevance and feasibility in humans remain uncertain. Recently, a few human cell–based in vitro studies have been reported, for example, Higgins et al. reported DP spheroids (DPS) by the hanging drop method that could at least partially restore few DP signature marker proteins, such as versican (VCAN), alkaline phosphatase (ALP), and β-catenin, which are either nominally expressed or absent in a two-dimensional (2D) monolayer culture (Higgins, Chen, Cerise, Jahoda, & Christiano, 2013). However, large nonuniformity in the results made this model questionable as VCAN expression was upregulated in only three of the eight cell lines tested. When DP cells were cultured over a poly(ethylene-covinyl alcohol; Young, Lee, Chiu, Hsu, & Lin, 2008) or a poly(vinyl alcohol) film (Huang, Chang, Aggarwal, Lee, & Ehrlich, 1993), the self-assembling characteristics of these cells led to the development of 3D aggregates, albeit aggregates with varied cell numbers and nonuniform size. Moreover, there might be a selective clonal population, where selected clones that are loosely attached may get washed out during media change. Another major problem is that DP cells lose their trichogenic characteristics after more than 10 passages in a 2D culture (Inamatsu, Matsuzaki, Iwanari, & Yoshizato, 1998). But cocultures of DP cells and keratinocytes could support the growth of the DP cells until 90 passages of culture (Inamatsu et al., 1998). Limat et al. (1993) reported enhanced growth of HF outer root sheath cells when cocultured with DP cells. However, the cocultured models of HF regeneration developed to date are mostly monolayer-based models and thus have failed to replicate several key features of the HF microenvironment.

Expression of Wnt proteins and Sonic hedgehog in the HF epidermal region is important to maintain DP cells in the anagen stage (Kishimoto, Burgeson, & Morgan, 2000). Hence, instead of viral-mediated gene transfer or exogenous addition to media, it would be interesting if one can trigger selected protein expression mediated by biomaterials. By coculturing murine origin HF epithelial cells and adipocytes in 3D collagen type I hydrogel, an HF organoid model was developed, in which adipocytes were found to play a role in controlling HF cell proliferation (Misago, Toda, Sugihara, Kohda, & Narisawa, 1998). Havlickova et al. highlighted the use of a sandwich model of HF using collagen type I and matrigel to understand complex epithelial–mesenchymal interactions (EMIs) involved during human HF development (Havlickova, Biro, Mescalchin, Arenberger, & Paus, 2004). However, these models suffer from inherent problems related to the materials, for example, collagen-based models show extensive contraction, whereas matrigel, being derived from murine sarcoma cells, may not be appropriate for the development of human cell–based HF models. To overcome these drawbacks, our strategy was to initially start with the development of a simple DPS model, followed by the development of a more sophisticated HF organoid model by encapsulating the DP spheroid by two types of cells (HF keratinocytes and HF stem cells) within a silk–gelatin (SG) hydrogel. We have previously reported the development of a cytocompatible silk fibroin protein and gelatin-conjugated hydrogel. The SG hydrogel could support long-term cell viability in a number of primary and stem cell populations (Das et al., 2015), provided an optimum 3D microenvironment for the immobilization of growth factors, supported remodeling of the pericellular matrix, and triggered the activation of Wnt–β-catenin signaling (Chameettachal, Midha, & Ghosh, 2016; Chawla, Kumar, Admane, Bandyopadhyay, & Ghosh, 2017; Chawla, Midha, Sharma, & Ghosh, 2018). Instead of random and heterotypic cellular aggregation (Yen, Chan, & Lin Sung Jan,

2010), a strategic and spatial placement of epithelial HF keratinocytes cells and HF stem cells in the SG hydrogel surrounding the mesenchymal DP aggregates might be advantageous to develop an anatomically relevant HF organoid model.

Hence, the aim of the current study is to establish a reproducible in vitro HF organoid model that simulates the following: (a) the intricate characteristics of the DP cluster, (b) complex EMIs, and (c) signaling pathways associated with in vivo HF development and could thus be used to test the efficacy of hair regeneration drugs. Toward this end, in the current study, we conducted a series of experiments: (a) development and characterization of a human DP cell–based spheroid model, (b) demonstration of the feasibility of using the DPS model to study the effect of hair regeneration medicine (minoxidil) through extensive gene expression profiling, (c) determination of the role of the SG hydrogel in modulating the DPS microenvironment and induce HF regeneration, and (d) determination of the effect of a coculture spheroid model of DP cells, human HF keratinocytes and HF stem cells, encapsulated in an SG hydrogel, in modulating the coculture spheroid model microenvironment. The insights from these simple human cell–based in vitro models will enable a systematic exploration of the dynamic regulatory mechanisms during self-assembly of DP aggregates and the surrounding cells to elucidate the signaling communication between the epithelial HF cells and mesenchymal DP cells, which could provide future avenues for HF regeneration and therapeutic interventions and present an alternative to animal model-based drug-screening methods.

2 | EXPERIMENTAL SECTION

2.1 | Cell culture and media compositions

Human HF DP cells (cat. no. C-12071; PromoCell) were expanded at a density of 6,000 cells/cm^2 in DP culture media (cat. no. C-26501; PromoCell) containing 2.5 μg/ml of amphotericin B (cat. no. A011; Himedia), 50 μg/ml gentamycin, 100 U/ml penicillin/streptomycin (cat. no. A001A; Himedia), and a supplement mix (cat. no. C-39625; PromoCell) containing 4% fetal calf serum, 1 ng/ml basic fibroblast growth factor, and 5 μg/ml recombinant human insulin. Human HF keratinocytes (K cells, cat. no. 2440; CellScience Cell) and human HF stem cells (S cells, cat. no. 36007-08; Celprogen) were expanded and cultured in specific media: keratinocyte media (cat. no. 27501; Celprogen) and human HF stem cells expansion media (cat. no. M320510-08S; Celprogen), respectively. Cells of passage numbers 4–6 were used for all experiments.

2.2 | Preparation of silk fibroin solution

Bombyx mori silk cocoons were provided by the Central Silk Board, Bangalore, Ministry of Textiles, Government of India. The stock solution of silk fibroin was prepared as mentioned in our previous studies (Chameettachal, Murab, Vaid, Midha, & Ghosh, 2015; Dubey, Murab, Karmakar, Chowdhury, & Ghosh, 2015). Briefly, 5 g of silk cocoons were cut into smaller pieces, boiled in 0.02 M Na_2CO_3 twice for 20 min, followed by rinsing in distilled water to remove sericin. The extracted fibers were dried overnight at 37°C and subsequently dissolved in 9.3 M LiBr solution (cat. no. 31665; SRL Pvt. Ltd.) kept at 60°C for 4 hr, leading to the development of 20% wt/vol of an aqueous silk fibroin solution. This resultant fibroin solution was dialyzed against deionized water using a Slide-a-Lyzer Dialysis Cassette (MWCO 3500; Pierce) for 48 hr to remove lithium bromide, resulting in a 5% wt/vol fibroin aqueous solution.

2.3 | Preparation of 3D DPS

Ninety-six-well U-bottomed plates were coated with 1% (wt/vol) poly-2-hydroxyethyl methacrylate (cat. no. P3932; Sigma-Aldrich; Ghosh et al., 2005). 2.5×10^4 DP cells were added per well to develop 3D DPS. The cell culture was carried out in a CO_2 incubator at 37°C and 5% CO_2. The diameter of the DPS was measured using ImageJ software (NIH).

2.4 | Experimental groups

The SG hydrogel was developed by adding 5 wt% of ethanol-sterilized gelatin (G2500; Sigma-Aldrich) powder to a 5% wt/vol autoclaved silk fibroin solution and enzymatic crosslinking was performed by adding 800 U/ml of tyrosinase (cat. no. T3824-50KU; Sigma-Aldrich; Chawla et al., 2017).

Four different experimental groups were tested in this study: (a) DPS; (b) a DPS (5×10^3 cells/spheroid) with 10 μM minoxidil (cat. no. M4145; Sigma-Aldrich) to test the feasibility of the drug-testing system; (c) DPS encapsulated with 5% wt/vol of a SG hydrogel (DPS-SG); (d) DPS encapsulated with HF keratinocytes and stem cells (DPS + KS, 5×10^3 cells each); and (e) DPS encapsulated with an SG hydrogel containing a coculture with HF keratinocytes and stem cells (5×10^3 cells; DPS + KS-SG). Cells cultured in the 2D monolayer were considered as controls for all the experiments.

2.5 | DNA content estimation

The genomic DNA was isolated using the DNA Isolation Kit (cat. no. G7505A; Agilent Technology) from the cells cultured in different experimental groups at specific time points. The DNA concentration was estimated using Nanodrop 2000C (Thermo Fisher Scientific, Wilmington, DE).

2.6 | Gene expression analysis by reverse-transcription polymerase chain reaction (RT-PCR)

RNA was isolated from the cells cultured in different experimental groups at specific time points using the RNA Isolation Kit (cat. no. 74106; Qiagen). The concentration and purity of isolated RNA were determined using Nanodrop 2000C Spectrophotometer (Thermo Fisher Scientific). The first-strand cDNA synthesis kit (cat. no. K1612; Thermo Fisher Scientific) was used to reverse-transcribe the RNA into complementary DNA using the first-strand cDNA synthesis kit. Quantitative RT-PCR was performed using SYBR Green Master Mix

(cat. no. 204074; Qiagen) and the Rotor Gene Q thermocycler (Qiagen; Chawla, Chameettachal, & Ghosh, 2015). QuantiTect Primers (Qiagen) listed in Table 1 were used for the gene expression analysis. Glyceraldehyde 3-phosphate dehydrogenase housekeeping gene expression was used for normalization and 2D monolayer Day 1 was considered the control for all the calculations. The relative expression levels were calculated using the $2^{-\Delta\Delta C_t}$ method.

2.7 | Immunofluorescence analysis

Ki-67 staining was performed for the DPS-SG, DPS + KS, and DPS + KS-SG groups to visualize and estimate the differences in the proliferation status. Immunofluorescence analysis for fibronectin (FN) was performed for all the experimental groups at specific time points. Spheroids in different experimental groups were washed with phosphate-buffered saline (PBS), followed by permeabilization using 0.1% Triton X-100 (cat. no. T878; Sigma-Aldrich), followed by blocking with 1% bovine serum albumin (BSA) (cat. no. A9418; Sigma-Aldrich). Incubation in the primary antibodies: fibronectin (1:200, 6328; Abcam), Ki-67 (1:100, 6526; Abcam), and actin phalloidin (1:50, 143533; Abcam) was performed for 1 hr at room temperature (RT) for the respective samples. After washing with PBS, spheroids were incubated with Alexa Fluor 546 goat antimouse IgG (1:200, A11030; Invitrogen) and Alexa Flour 488–conjugated goat antimouse IgG antibody (1:200, A11001; Invitrogen) for 1 hr at RT. DAPI (cat. no. 32670; Sigma-Aldrich) was used for nuclear staining. Actin phalloidin staining and FN staining were performed for DPS with and without minoxidil. Images were acquired using a Leica TCS SP5 (Leica Microsystems) inverted confocal laser scanning microscope. The mean fluorescence intensity was quantified using Python image analysis (Chawla & Ghosh, 2018).

2.8 | Live–dead staining

Spheroids from DPS + KS and DPS + KS-SG were stained to detect viable cells using a Live/Dead Staining Kit (Invitrogen) at Day 21 using 4 μM ethidium homodimer and 2 μM calcein. Images were acquired using a Leica TCS SP5 (Leica Microsystems) inverted confocal laser scanning microscope (Chawla & Ghosh, 2017). The percentage of live and dead cells was calculated using ImageJ software (NIH; Chawla et al., 2017).

2.9 | Histological analysis

Spheroids from the DPS-SG and DPS + KS-SG group were collected at different time points and washed with PBS and fixed in 4% formaldehyde for 1 hr at RT. Eight-micrometer-thick sections were collected on coated slides and stained with hematoxylin and eosin (H&E) to study the cell morphology. Cell number and morphology in the inner and outer zone were calculated using ImageJ software (NIH).

2.10 | Statistical analysis

Results were expressed as mean–standard errors of at least three replicates. Data were analyzed using one-way analysis of variance,

TABLE 1 List of primers used for gene expression analysis

Serial no.	Description	Gene name	Cat. no.
1	FN	Fibronectin	QT00038024
2	SPARC	Secreted protein acidic and rich in cysteine	QT00018620
3	VCAN	Versican	QT00064064
4	ALP	Alkaline phosphatase	QT00211582
5	BMP2	Bone morphogenetic protein-2	QT00012544
6	BMP4	Bone morphogenetic protein-4	QT00012033
7	CTNNB-1	β-Catenin	QT00077882
8	HIF1α	Hypoxia-inducible factor 1-α	QT00083664
9	RUNX2	Runt-related transcription factor 2	QT00020517
10	NOG	Noggin	QT00210833
11	VEGF	Vascular endothelial growth factor	QT00198954
12	GAPDH	Glyceraldehyde 3-phosphate dehydrogenase	QT00079247

Note. STRING V 10.0 (search tool for the retrieval of interacting genes–proteins) was used (http://string-db.org/; Murab et al., 2013) to study the possible protein–protein interactions between the proteins expressed by the studied set of genes for each condition.

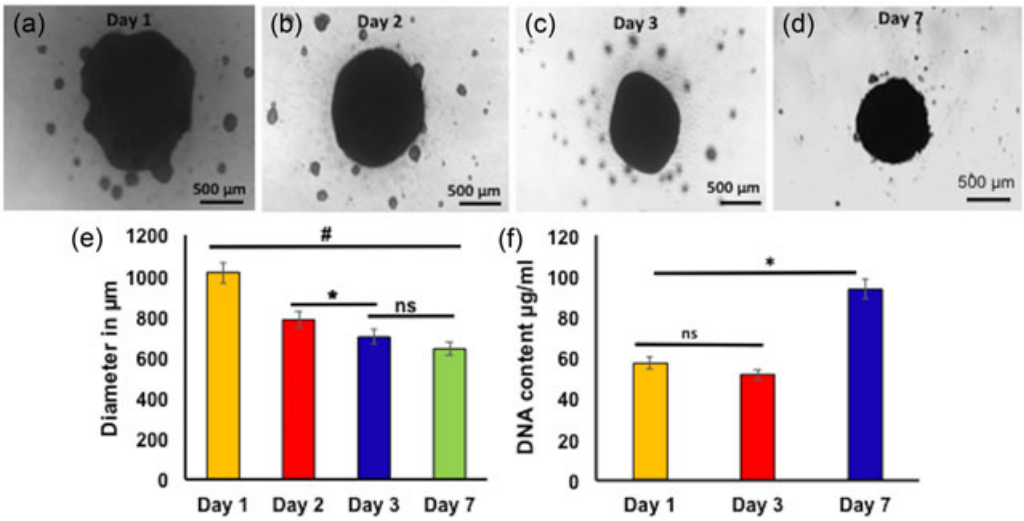

FIGURE 1 Dermal papilla spheroids (DPS) formation and size analysis. 2.5×10^4 DP cells cultured on poly-(2-hydroxyethyl methacrylate)-coated 96-well U-bottomed plates showing irregular cellular aggregation at Days 1 and 2 (a,b) and floating unified DP sphere formation at Days 3 and 7 (c,d). Sphere size (µm) as calculated by measuring the approximate diameter of individual spheres at Days 1, 2, 3, and 7 (e). Total DNA content of DPS measured at Days 1, 3, and 7 (f). Values are mean ± *SD*; $n = 8$/group. $^*p \le 0.01$ and $^\#p \le 0.001$. Scale bars = 500 µm [Color figure can be viewed at wileyonlinelibrary.com]

followed by the Bonferroni post hoc test. The statistical significance $p \le 0.01, 0.001, 0.0001$ was considered significant wherever applicable.

3 | RESULTS

3.1 | Development and characterization of 3D DPS

DP cells were cultured in a poly-(2-hydroxyethyl methacrylate)-coated 96-well plate, started aggregation with irregular and maintained their shape thereafter (Figure 1d). The diameter of the spheroids decreased significantly from 1,014 ± 68 µm on Day 1 to 785 ± 33 µm Day 2 ($p < 0.01$) and further declined to 699 ± 41 µm at Day 3 ($p < 0.001$; Figure 1e). No significant reduction in the spheroid size was observed thereafter at Day 7, with a spheroid size of 635 ± 24 µm (Figure 1e). However, the DNA content increased from Days 1 to 7 (Figure 1f), indicating that there was no or insignificant cell death and the decline in the size of the spheroid was due to compaction mediated by homotypic cell adhesion. Further increase in the DNA content by Day 7 (significant at $p < 0.01$) indicated continued cell proliferation inside the 3D spheroid system.

Expression of a constellation of DP-specific marker genes, namely, FN, secreted protein acidic and rich in cysteine (SPARC), VCAN, ALP, BMP2 and BMP4, hypoxia-inducing factor 1 α (HIF1α), and β-catenin, was assessed at different intervals of cultured DPS. We observed an increase in the expression of ECM-specific genes, namely, FN (3.3-fold, significant at $p < 0.001$; Figure 2a-i), SPARC (3.2-fold, significant at $p < 0.001$; Figure 2a-ii), and VCAN (2.2-fold, significant at $p < 0.01$; Figure 2a-iii) from Days 3 to 7, indicating enhancement in the ECM production by the cultured cells in 3D spheroids. Although ALP has been reported to be a marker of DP aggregation and proliferation (Lee et al., 2012), we observed negligible ALP expression in our DPS model. Moreover, its expression level did not significantly modulate throughout the culture time points (Figure 2a-iv). To elucidate the involvement of BMP and canonical Wnt–β-catenin, we checked the expression of these two markers in the developed DPS. Nominal expression (<1-fold) of BMP2 (Figure 2a-v) and BMP4 (Figure 2a-vi) was observed in DPS throughout the culture time points. The expression of β-catenin increased significantly from Days 3 to 7 (Figure 2a-vii), indicating the involvement of the canonical Wnt–β-catenin pathway in the DPS.

We also observed that the expression of HIF1α increased significantly from Days 3 to 7 (73.6-fold, $p < 0.001$; Figure 2a-viii) in our DPS model. STRING analysis further revealed a high level of interaction among the studied set of genes, with two to three genes involved per pathway in the involvement in HF (Figure 2b). These findings highlighted the relevance of our developed in vitro DPS model of HF regeneration with in vivo HF regeneration. An immunofluorescence (IFC) analysis was performed to validate the expression of FN in the DPS. We observed prominent expression of FN in both the 2D monolayer (Figure 3a,b) and the DPS on Day 3 (Figure 3c–e) and Day 7 (Figure 3f–h). However, the measured mean fluorescence intensity value of FN in the DPS was significantly higher ($p < 0.001$) than the 2D monolayer (Figure 3i), indicating higher FN expression by the cells in 3D DPS compared with 2D. Moreover, there was a significant increase ($p < 0.001$) in the mean fluorescence intensity of FN from Days 3 to 7 of DPS, which validated the gene expression data.

3.2 | Effect of minoxidil on DP-specific gene expression

A comparative gene expression analysis was performed at 12 and 24 hr of minoxidil treatment compared with the control DPS without any treatment to compare the expression of ECM-specific genes FN, SPARC, and VCAN, and ALP as a measure of metabolic activity,

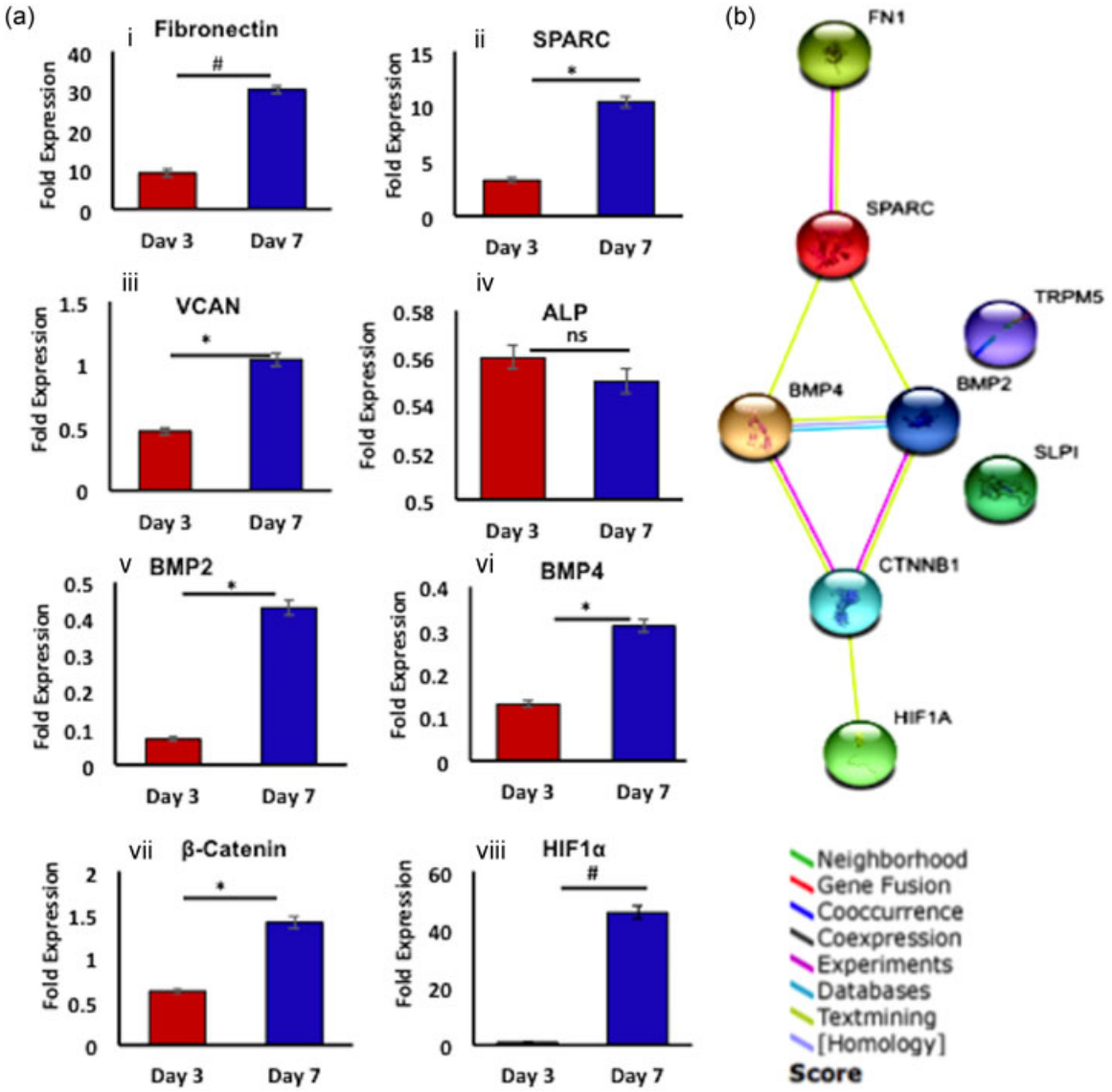

FIGURE 2 (a) Dermal papilla (DP)–specific signature gene expression analysis of cultured DP spheroids (DPS) at Days 3 and 7: i, FN; ii, SPARC; iii, VCAN; iv, ALP; v, BMP2; vi, BMP4; vii, β-catenin; and viii, HIF1α. (b) Protein–protein interactions studied using STRING analysis showed closed similarity of the developed in vitro DPS with in vivo HF. ALP, alkaline phosphatase; BMP2, bone morphogenetic protein-2; BMP4, bone morphogenetic protein-4; FN, fibronectin; HF, hair follicle; HIF1α, hypoxia-inducible factor 1-α; SPARC, secreted protein acidic and rich in cysteine; VCAN, versican [Color figure can be viewed at wileyonlinelibrary.com]

hypoxia-specific HIF1α and signaling pathway–specific genes BMP2, BMP4, and β-catenin for all three groups. Significantly upregulated FN expression was observed in minoxidil-treated DPS at 12 and 24 hr compared with the control (Figure 4a). The expression of SPARC (Figure 4b), VCAN (Figure 4c), and ALP (Figure 4d) showed a similar profile, where upregulated expression of all these genes was observed at both 12 hr (not significant) and 24 hr (significant at $p < 0.01$). Nominal levels of BMP2 (Figure 4e) and BMP4 (Figure 4f) expression could be observed at 12 hr of minoxidil treatment. BMP2 expression levels declined at 24 hr, whereas constant levels of BMP4 expression were maintained. Upregulated expression of β-catenin was observed after 12 hr of minoxidil addition (1.8-fold higher compared with the control DPS, significant at $p < 0.01$), which increased further by 24 hr (3.8-fold higher than the control DPS, significant at $p < 0.001$; Figure 4g). The expression of runt-related transcription factor 2 (RUNX2; Figure 4i), vascular endothelial growth factor (VEGF; Figure 4j), and HIF1α (Figure 4h) decreased after 12 hr of minoxidil addition compared with the control DPS; however, there was an increase in the expression after 24 hr (significant changes at $p < 0.01$ for RUNX2, but not significant for VEGF and HIF1α).

To further validate the expression of FN, immunofluorescence analysis showed prominent expression of FN in all the groups (Figure 5). However, minoxidil-treated DPS showed enhanced FN expression (measured as the mean fluorescence intensity differences) at both 12 hr (Figure 5g) and 24 hr (Figure 5o) compared with the control. We also studied the differences in the actin expression after the treatment of DPS with minoxidil. No notable difference was observed in the

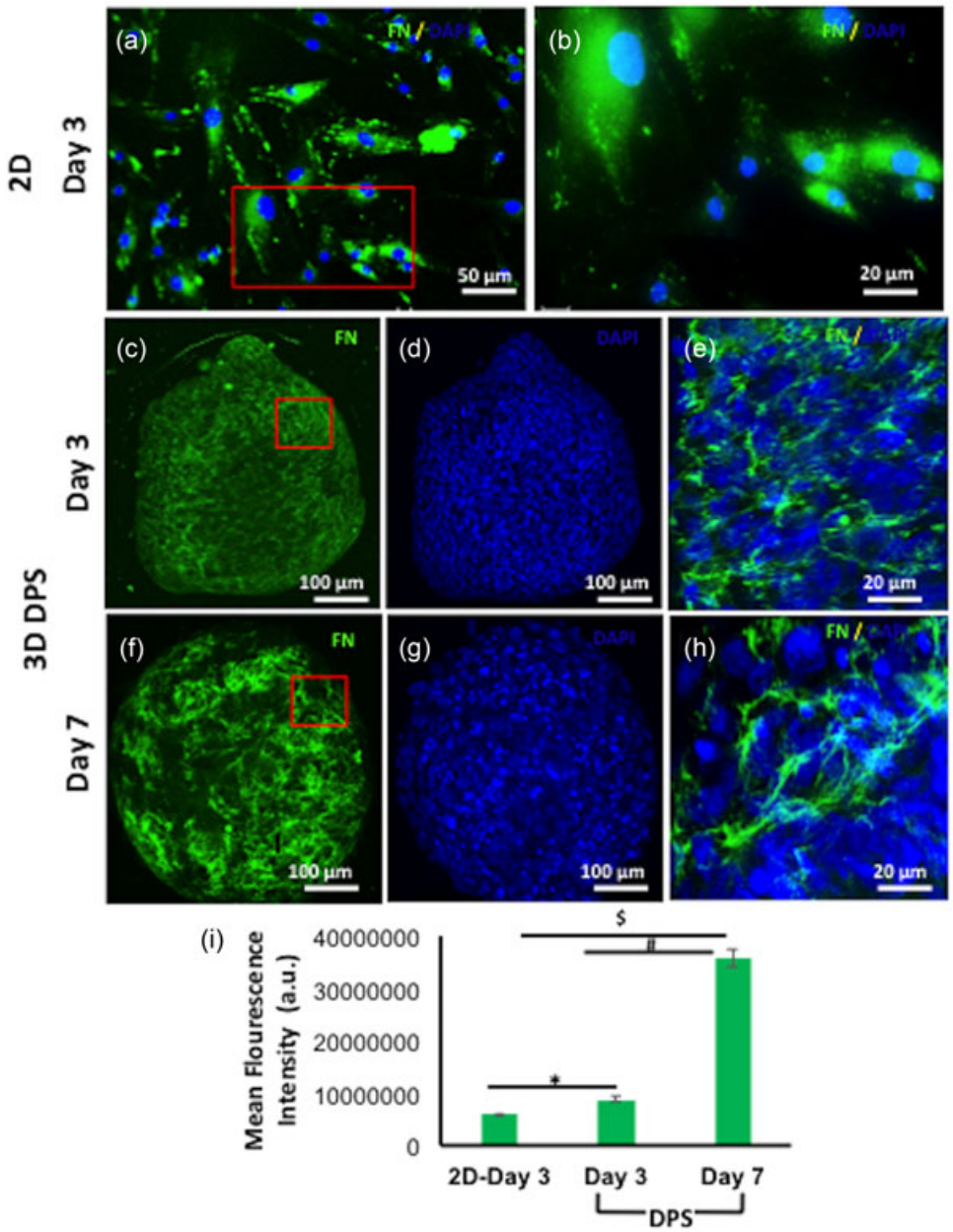

FIGURE 3 Fibronectin expression in 2D versus 3D dermal papilla spheroids (DPS). 2D culture showing DP cells immunostaining of fibronectin (green) and DAPI (blue) (a) and magnified view (b). Fibronectin expression on DPS (c), nuclear stain DAPI (d), and magnified view (e) at Days 3 and 7 (f,g,h). Mean fluorescence intensity of fibronectin of individual DPS at Days 3 and 7 as compared to the 2D (i). *$p \leq 0.01$. Values are mean ± *SD*; $n = 7$ images (region of interest)/group. 2D, two-dimensional; 3D, three-dimensional [Color figure can be viewed at wileyonlinelibrary.com]

control and 12-hr minoxidil-treated DPS; however, interestingly, at 24 hr, the expression of actin was limited to the periphery of the spheroids (the control DPS) compared with the uniform actin distribution in the minoxidil-treated DPS.

3.3 | Modulation of the developed DPS model toward the development of the HF organoid model

To evaluate the state of proliferation of DPS with or without the presence of SG and/or coculture of keratinocytes and stem cells, immunohistochemical staining for anti-Ki-67, a proliferation-associated marker, was performed. We observed prominent expression of Ki-67 in all the groups at Day 7, indicating that cells were actively proliferating throughout the entire DPS (Figure 6a). However, the measured mean fluorescence intensity value was the highest (significant at $p < 0.0001$) in the DPS + KS-SG, group followed by the DPS + KS, DPS-SG, and DPS groups (Figure 6b), indicating higher cellular proliferative activity in the coculture system in the presence of SG matrix compared with only DPS. Further, the live–dead analysis revealed around 92% live cells in DPS + KS-SG compared with 64% live cells in DPS + KS at Day 21 (Figure 6c). The DPS + KS-SG group showed the highest DNA content (significant at $p < 0.001$), followed by the DPS-SG and DPS + KS groups (Figure 6d).

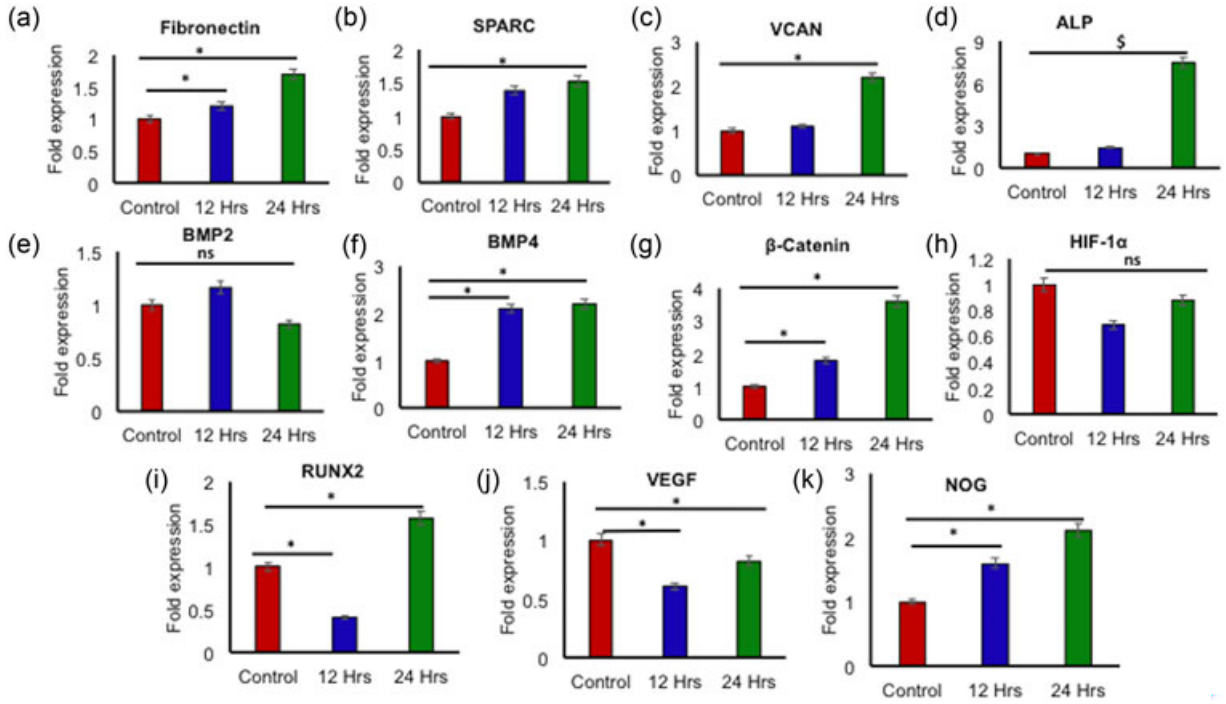

FIGURE 4 Differential gene expression profile of dermal papilla spheroids (DPS) treated with 10 μM minoxidil at 12 and 24 hr as compared to the control DPS. Symbols * and $ indicate significance $p \leq 0.01$ and 0.001, respectively. ALP, alkaline phosphatase; BMP2, bone morphogenetic protein-2; BMP4, bone morphogenetic protein-4; HIF1α, hypoxia-inducible factor 1-α; NOG, noggin; RUNX2; runt-related transcription factor 2; SPARC, secreted protein acidic and rich in cysteine; VCAN, versican [Color figure can be viewed at wileyonlinelibrary.com]

A comparative gene expression analysis was performed for the DPS-SG, DPS + KS, and DPS + KS-SG groups at Day 7. The DPS + KS-SG group showed the highest expression of all the ECM-specific genes FN compared with the DPS-SG (1.2-fold, significant at $p < 0.01$) and DPS + KS groups (1.4-fold, significant at $p < 0.01$; Figure 7a-i). The SPARC (Figure 7a-ii) and VCAN (Figure 7a-iii) groups followed a similar pattern, where the highest expression of both the genes was observed in the DPS-SG + KS group compared with the DPS-SG (1.9-fold for SPARC, significant at $p < 0.001$, and 1.3-fold for VCAN, significant at $p < 0.01$) and DPS + KS (1.4-fold for SPARC, significant at $p < 0.001$ and 3.9-fold for VCAN, significant at $p < 0.001$). The DPS + KS-SG group showed the highest expression of ALP compared with the DPS-SG (1.6-fold, significant at $p < 0.01$) and DPS + KS groups (1.9-fold, significant at $p < 0.001$; Figure 7a-iv). The expression of β-catenin showed maximum upregulation in the DPS + KS-SG group compared with DPS-SG (3.4-fold, significant at $p < 0.001$) and DPS + KS (1.4-fold, significant at $p < 0.01$) groups, indicating the involvement of the canonical Wnt–β-catenin signaling pathway in the DPS + KS-SG group (Figure 7a-vii).

Significantly elevated expression of HIF1α was observed in the DPS + KS-SG group followed by the DPS + KS and DPS-SG groups (3.3-fold, $p < 0.001$; Figure 7a-viii). We could exclude the possibility of induction of hypoxia due to the limited diffusibility and mass transfer in the SG hydrogel as the DPS-SG showed the least HIF1α gene expression. The IFC analysis further validated the gene expression analysis as prominent expression of FN was observed in all the three groups: DPS-SG, DPS + KS, and DPS + KS-SG (Figure 7b). However, the measured mean fluorescence intensity value of FN in the DPS + KS-SG was significantly higher than that of the DPS + KS (1.9-fold, $p < 0.001$) and DPS-SG (4.9-fold, $p < 0.001$; Figure 7c) groups, which is in line with the gene expression pattern of FN as observed in the gene expression analysis.

Further, to visualize the spatial distribution of cells and further clarify the cellular characteristics within the DPS-SG and DPS + KS-SG groups, H&E staining was done at Day 7. Examination of the histological sections revealed the presence of an outer zone and an inner zone within the spheroids (Figure 8a) of the DPS-SG group. Relatively large and spindle-shaped nuclei were observed in the DP cells under high magnification in the outer zone, whereas the inner zone showed rounded or oval nuclei (Figure 8a-iii,d). We also found extensive ECM deposition in the spheroids of the DPS-SG (Figure 8a) and DPS + KS-SG groups (Figure 8c). A higher number of cells were evident in the outer zone spheroids of the DPS-SG group compared with the inner zone.

4 | DISCUSSION

Most of the recent reports on hair regeneration have used either rodent cells, from newborn or embryonic mice (Ehama et al., 2007) or via grafting of human and rodent dermal cells in vivo (Toyoshima et al., 2012). An ideal model for human cell–based HF regeneration that can successfully replicate the complex microenvironment involved in in vivo hair regeneration is yet to be developed. To the best of our knowledge, this is the first study suggesting that the

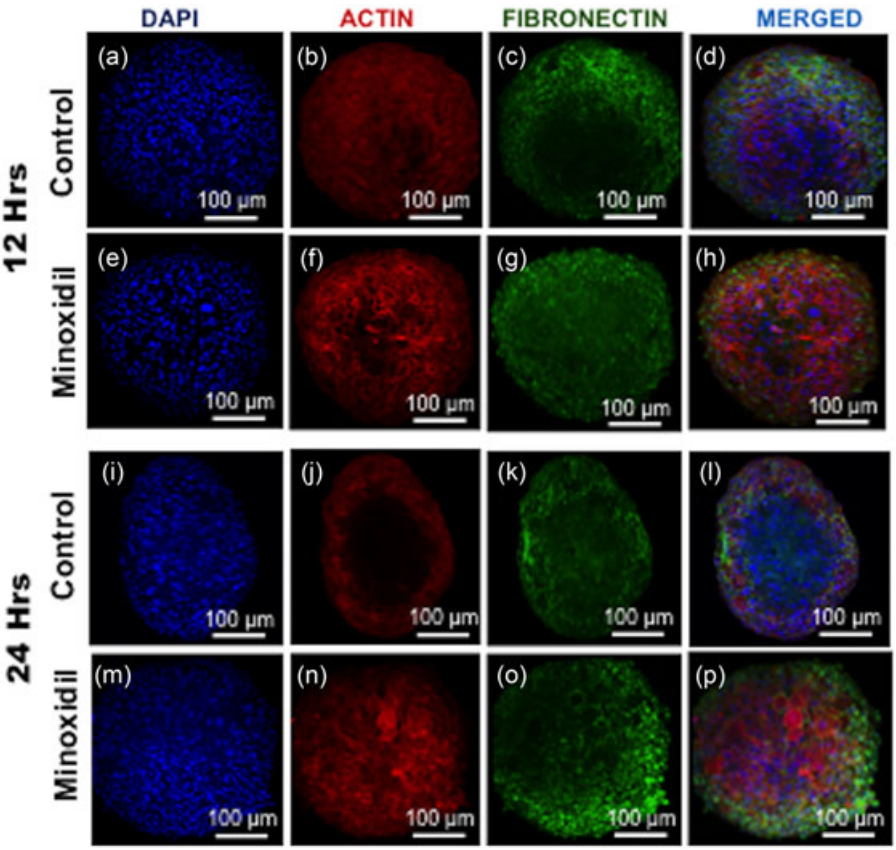

FIGURE 5 Fibronectin and actin expression on dermal papilla spheroids (DPS) treated with minoxidil (10 µM). Alexa Flour 488 antibody (green) for fibronectin, phalloidin (red) for actin and DAPI (blue) nuclear staining at 12 hr (a–h) and 24 hr (i–p) of culture. Scale bars represent 100 µm [Color figure can be viewed at wileyonlinelibrary.com]

spatial organization of DPS, HF keratinocytes, and stem cells of human origin cocultured in a spatially organized manner in an inductive microenvironment offered by a SG hydrogel represents a viable approach to establish an in vitro model of HF neogenesis.

An in vivo DP matrix is known to possess a high amount of FN and SPARC (Messenger et al., 1991; Soma, Tajima, & Kishimoto, 2005; Won et al., 2012). The gene expression of FN, SPARC, and VCAN in our DPS model showed relevance to in vivo system. VCAN is an important marker of the early-stage anagen phase of HF development (Soma et al., 2005). The upregulated expression of VCAN in vitro showed that our DPS model could recapitulate, at least to some extent, the characteristic feature of the growth phase of in vivo HF development. Further, upregulated β-catenin activity has been observed in the growing anagen stage of HF development in murine models (Maretto et al., 2003), whereas inhibition of β-catenin leads to premature activation of the catagen phase in vivo (Enshell-Seijffers, Lindon, Kashiwagi, & Morgan, 2010). Human DP cells lose their HF-inductive property when cultured in the absence of Wnt–β-catenin signaling (Soma, Fujiwara, Shirakata, Hashimoto, & Kishimoto, 2012). The upregulated expression of β-catenin indicates the probable involvement of the Wnt–β-catenin pathway in our in vitro system. Regulation of BMP signaling has been linked to the modulation of the quiescent perifollicular microenvironment to a positive state responsive to HF regeneration by the activation of Wnt signaling (Jahoda & Christiano, 2011). Thus, it was interesting to note that in our model, mere 3D aggregation of DP cells could induce BMP inhibitory signals and could simultaneously upregulate β-catenin gene expression, which have been observed in vivo in enhanced induction of HF regeneration and DP-specific ECM expression (Maretto et al., 2003). The highly upregulated expression of HIF1α could be a possible indication of the activation of VEGF and Akt signaling pathways since HIF1α is the main factor involved in the initiation of hypoxia that potentiates the activation of VEGF and Akt, and thus induces the physiologic growth of HF in vivo (Rosenberger et al., 2007).

Through this study, we also aimed to demonstrate the feasibility of evaluating the effects of a test molecule using this simple in vitro DPS model system by assessing the gene expression of the signature marker of DP cells and markers associated with signaling pathways specific to HF regeneration. Minoxidil was selected as the model drug due to its known role in inducing HF regeneration. Minoxidil acts as a vasodilator to enhance blood flow to the DP (Headington, 1987), triggers secondary progression of the telogen to the anagen stage of follicles (Mori & Uno, 1990), and opens up intracellular potassium channels (Davies et al., 2005). In our study, minoxidil could promptly modulate the expression of DP-specific signature genes and enhanced the production of ECM compared with the control DPS. This is in agreement with the earlier reports where minoxidil has been known to induce phosphorylation of protein kinase B (Akt) and extracellular signal-regulated kinase signaling pathways eventually leading to upregulation of ECM genes in human DP cells (Han et al., 2004). Further, the upregulated expression of RUNX2 on the addition of minoxidil further confirmed the competency of our DPS model since RUNX2 plays a significant regulatory role in the development of HF through regulation of hedgehog signaling (Glotzer, Zelzer, & Olsen, 2008). ALP is another crucial marker for the activation of hair growth

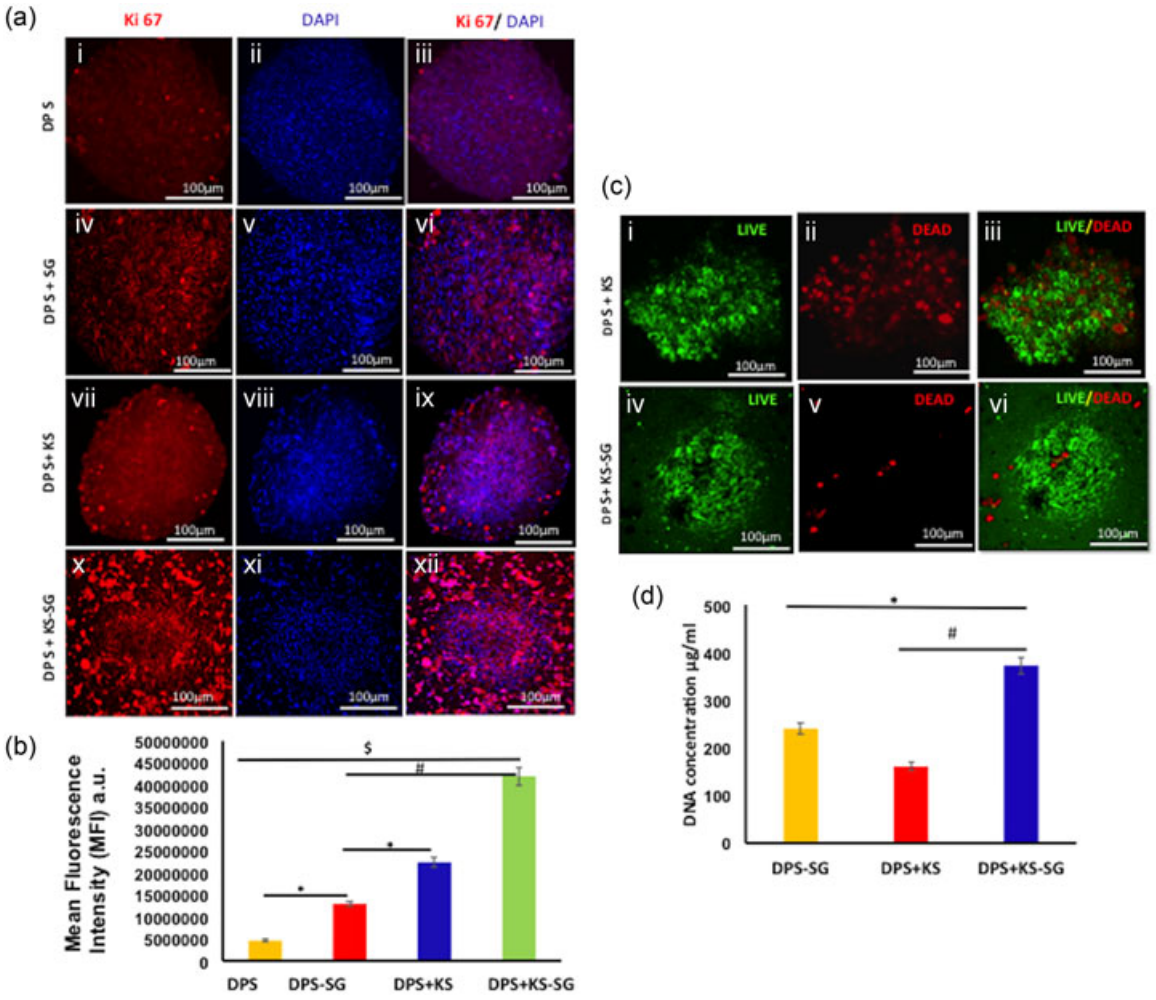

FIGURE 6 Expression of Ki-67 in dermal papilla spheroids (DPS) and DPS with silk–gelatin (DPS-SG), DPS cocultured with human hair follicle (HF) keratinocytes and human HF stem cells (DPS + KS) with and without SG (DPS + KS-SG) at Day 7 Alexa Fluor 546 (red) for Ki-67 and DAPI (blue) nuclear stain (a). Mean fluorescence intensity of Ki-67 for different groups at Day 7 (b). Live–dead cell imaging of DPS + KS and DPS + KS-SG at Day 21 (c). Scale bars = 100 µm. DNA estimated in DPS-SG, DPS + KS, and DPS + KS-SG at Day 7 (d). *$p \leq 0.01$. Values are mean ± *SD*; $n = 7$ images (region of interest)/group [Color figure can be viewed at wileyonlinelibrary.com]

in vivo (Müller-Röver et al., 2001). The significantly upregulated ALP gene expression levels on the addition of minoxidil to our DPS model confirmed that the minoxidil treatment was successful in activating the anagen hair regeneration stage in vitro. The role of the Wnt–β-catenin pathway has been identified in the activation of ALP activity in a murine model (Lee et al., 2012). We observed a similar correlation in the upregulated levels of ALP and β-catenin after 24 hr of minoxidil addition. In contrast to our finding, where VEGF expression did not show any change, Lachgar et al. showed increased VEGF expression on treatment of DP cells with minoxidil (Lachgar, Charveron, Gall, & Bonafe, 1998). We cannot exclude the possibility that higher concentrations of minoxidil may be required to induce VEGF expression. Rufaut et al. (2013) reported a dose-dependent reduction in the size of the DPS using lithium chloride, and minoxidil could reverse this size reduction by inducing the proliferation of the DP cells, but a detailed analysis of the changes in signaling pathways was not performed. We observed an upregulated expression of BMP2 and BMP4 at 12 hr of minoxidil addition in our DPS model. Once the DP cells enter the anagen stage, there is a neutralization of BMP by NOG signaling, with the simultaneous upregulation of Wnt–β-catenin signaling (Plikus, Widelitz, Maxson, & Chuong, 2009). We observed a similar temporal expression of NOG at 24 hr that possibly led to BMP inactivation and activated Wnt–β-catenin signaling (as observed by the four-fold upregulated expression of β-catenin). The importance of NOG expression in the activation of HF-inductive properties has been reported earlier (Botchkarev et al., 2002), where the induction of HF was compromised on deleting NOG from the system (Botchkarev et al., 1999). Further, upregulated β-catenin expression has been observed in both an in vivo mice model (Jun-Bo et al., 2007) and an in vitro human DP cell–based system (Kwack, Kang, Kim, Kim, & Sung, 2011), where activated β-catenin activity was linked to the extension of the anagen phase of HF. Thus, the similar upregulated expression of β-catenin on the addition of minoxidil in our DPS model is indicative of prolonged anagen phase in our system, which was further validated by the upregulated expression of anagen phase–specific ECM genes. Another interesting observation was the expression of actin in the

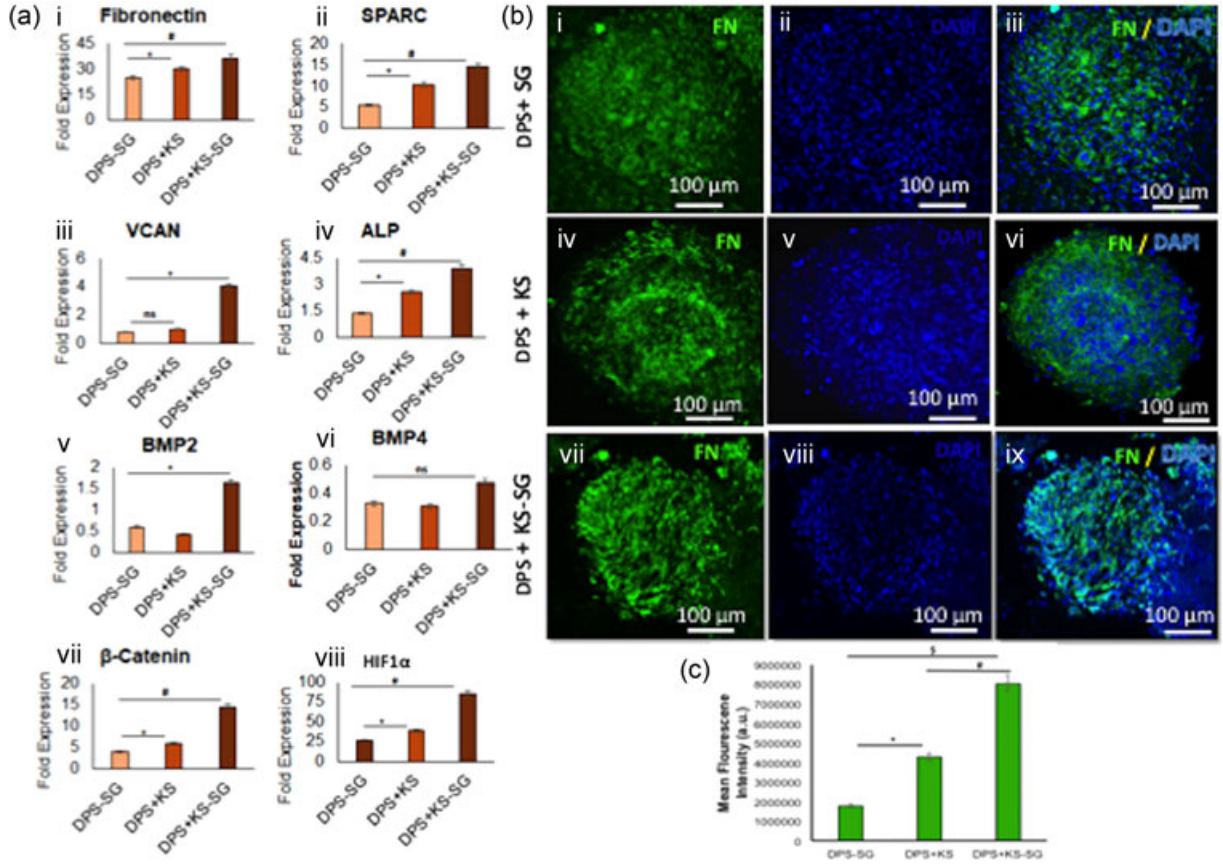

FIGURE 7 (a) Dermal papilla (DP)–specific signature gene expression analysis of DP spheroids with silk–gelatin (DPS-SG), DPS cocultured with human hair follicle (HF) keratinocytes and human HF stem cells (DPS + S) with and without SG (DPS + KS-SG) at Day 7: i, FN; ii, SPARC; iii, VCAN; iv, ALP; v, BMP2; vi, BMP4; vii, β-catenin; and viii, HIF1α. Expression of fibronectin on DPS-SG, DPS + cocultured with HF keratinocytes and stem cells (DPS + KS) with and without SG (b) Alexa Fluor 488 (green) for FN and DAPI (blue) nuclear stain. Mean fluorescence intensity of FN for different groups at Day 7 (c). Scale bars = 100 µm. *$p \leq 0.01$, #$p \leq 0.001$. ALP, alkaline phosphatase; BMP2, bone morphogenetic protein-2; BMP4, bone morphogenetic protein-4; HIF1α, hypoxia-inducible factor 1-α; SPARC, secreted protein acidic and rich in cysteine; VCAN, versican [Color figure can be viewed at wileyonlinelibrary.com]

DPS model, where actin was observed to be expressed only in the cells of periphery in the control DPS. However, minoxidil treatment helped to stabilize the expression of actin, with expression of well-characterized bundles of actin throughout the DPS, similar to the in vivo growth stage of HF regeneration (Furumura & Ishikawa, 1996).

A simplified organoid culture system of HF should preferably recapitulate the essential EMIs during human HF development (Havlickova et al., 2004). In human HF, DP cells are well assembled into a spatial 3D organization, wherein a DP cell does not operate in solitary, but is a part of the HF niche consisting of HF keratinocytes, stem cells, and many other cell types, which provide cues for DP to take up the function of producing hair shaft (Fujie, Katoh, Oura, Urano, & Arase, 2001; Jahoda, Horne, & Oliver, 1984; Oliver, 1967, 1970). The ECM microenvironment of these multiple cell types encompasses several molecular and physiological signals in an extensive network of macromolecules, for example, (a) proteoglycans, fibrillar collagens, and structural proteins such as FN, laminin, and elastin; (b) soluble cytokines and growth factors; and (c) surface proteins of the surrounding cells. Inclusion of HF keratinocytes with DP cells has been observed to significantly influence the induction of HF neogenesis through replication of the EMIs (Havlickova et al., 2004). Further, inclusion of stem cells helps in inducting an enhanced DP-specific ECM synthesis, with concomitant activation of HF development (Hsu et al., 2011). Thus, after successfully developing the DPS model, we attempted to further improve the model by encapsulation with SG hydrogel and by incorporation coculture of HF keratinocytes and stem cells within the hydrogel. The Ki-67 staining and live–dead analysis clearly highlighted the putative beneficial role of the coculture of cells and the surrounding SG matrix in DPS-SG and DPS + KS-SG spheroids in inducing enhanced cellular proliferation of the multiple cell types.

The upregulated expression of HF-specific ECM genes in the developed coculture DPS + KS and DPS + KS-SG models compared to single cell–based DPS offered a clear indication of DP-inductive properties for HF regeneration based on replication of the significance of EMI in DPS + KS and DPS + KS-SG-based HF organoid models. For example, significantly upregulated gene expression levels of VCAN in DPS + KS and DPS + KS-SG as compared with DPS are an important indicator of such biomimetic simulation of EMI in our coculture-based organoid model. VCAN is an essential regulator of EMI, which maintains HF-inductive properties during the early anagen stage, but disappears in the mid-to late stages. VCAN-positive epithelial and

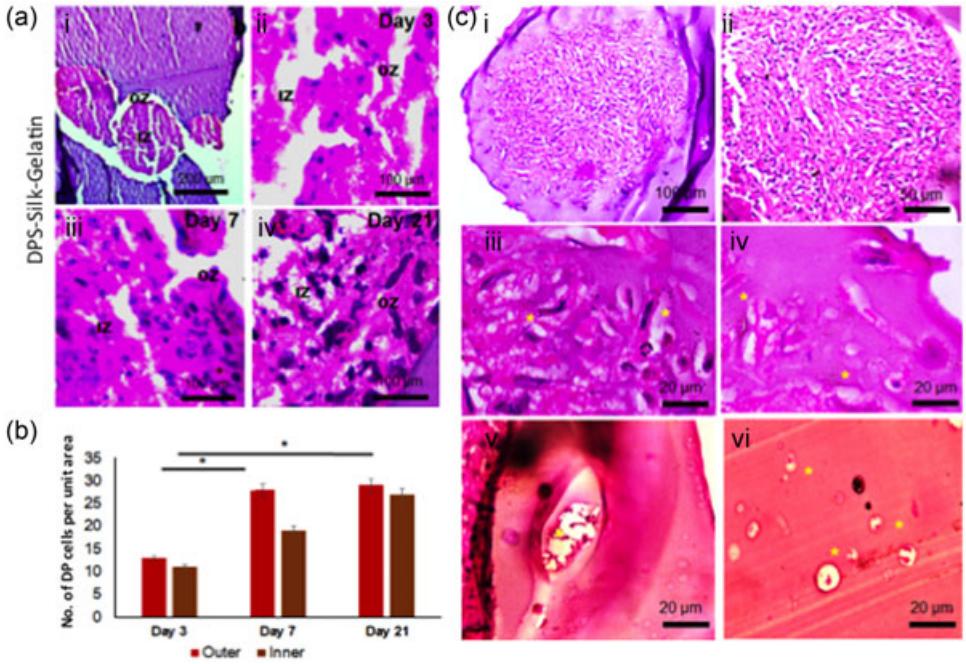

FIGURE 8 Histological analysis showing evidence of proliferation of dermal papilla spheroids (DPS) in silk–gelatin (DPS-SG) microenvironment at Days 3, 7, and 21 (a). Quantitative analysis shows significant difference in cell number at Days 3, 7, and 21 as well as difference in the morphology of the cells in the inner zone (IZ) and outer zone (OZ) of the spheroid (b) values are mean ± *SD*; region of interest from individual spheroids analyzed $n = 6$/group. (c) DPS cocultured with HF keratinocytes and stem cells at Day 7. $^*p \leq 0.01$ [Color figure can be viewed at wileyonlinelibrary.com]

mesenchymal cells alone have been reported to be sufficient for creating HF-inductive properties in vitro (Botchkarev & Kishimoto, 2003). Further, the increase in ALP expression in the DPS + KS model, compared with the negligible expression in DPS, is another indicator of enhanced HF-inductive properties leading toward in vivo like EMI contributed by the HF keratinocytes and stem cells. The results are in agreement with the in vivo HF development since an upregulated expression of ALP has been observed in DP in the anagen phase of hair growth (Iida, Ihara, & Matsuzaki, 2007).

BMP2 and BMP4 are important regulatory signaling effectors of the BMP signaling pathway that plays a significant role in maintaining the quiescent stage of the HF cycle. For HF to enter a proliferatory anagen phase, BMP inhibitors are expressed, which triggers the induction of growth and proliferation of HF (Solanas & Benitah, 2013). Thus, low levels of BMP2 and BMP4 expression in HF organoid models (DPS + KS and DPS + KS-SG) are indicative of a potentially favorable niche for HF regeneration. A signaling loop involving the Wnt–β-catenin pathway in both mesenchymal and epithelial niche cells has been identified to direct the synchronized EMI to steer the HF regeneration process (Enshell-Seijffers et al., 2010). Coculture of DP cells with epithelial and mesenchymal progenitor cells in the monolayer has been reported to enhance Wnt–β-catenin signaling (Chan, Fan, Wang, Mu, & Lin, 2015). However, the monolayer cell culture condition fails to recapitulate the closed microenvironmental niches that are required for HF growth and regeneration. In that context, the in vitro HF organoid model (DPS + KS and DPS + KS-SG) developed by us would certainly help to simulate such a 3D HF microenvironment. The upregulated expression of β-catenin in the HF organoid model substantiates the involvement of Wnt–β-catenin signaling in steering the EMI toward enhanced ECM production, extended proliferation and recapitulation of the HF microenvironment.

The upregulated expression of HF-specific ECM genes in the developed DPS + SG and DPS + KS-SG also offered a clear indication of enhanced DP-inductive properties by SG hydrogel. This could be attributed to the unique ability of the SG matrix to further enhance the synthesis of ECM in DPS-SG and DPS + KS-SG, probably due to the immobilization of the secreted growth factors and other effector biomacromolecules, thus replicating the hydrated microenvironment of DP (Kishimoto et al., 2000; Rendl, Polak, & Fuchs, 2008). Interestingly, the expression of β-catenin in the coculture model (DPS + KS) further increased significantly when the HF keratinocytes and HF stem cells were mixed with the SG hydrogel before DPS encapsulation (DPS-KS + SG). Overexpression of β-catenin signaling in vivo led to induction of DP condensate formation and HF morphogenesis (Chen, Jarrell, Guo, Lang, & Atit, 2012). Similar to such in vivo reports our findings highlight the instructive role of the microenvironment offered by the SG hydrogel by providing additional possibilities to modulate signaling pathways (Wnt–β-catenin pathway in this case) in dermal condensates and for capturing the essential EMI akin to in vivo hair regeneration.

Furthermore, another interesting observation was the increased transcript level of HIF1α observed in DPS + KS-SG that might have promoted the interaction of the cocultured cell population with the SG hydrogel further enhancing the possibilities of in vivo like simulation of EMI. Hypoxia-induced HIF1α expression in mammalian embryonic stem cells has been known to increase the proliferatory and migratory

properties of the cultured stem cells (Lee, Lee, & Han, 2011). The response is mediated by enhanced phosphorylation of mammalian target of rapamycin and increased activity of the phosphatidylinositol 3 kinase (P13K)/Akt pathway. Further, hypoxia has been observed to enhance growth factor secretion in a coculture monolayer model of adipose-derived stem cells, DP cells, and epithelial keratinocytes (Park et al., 2010). In our study, we observed upregulated HIF1α expression in the coculture model (DPS + KS, and DPS + KS-SG) compared with only the DPS model. This is indicative of the role of hypoxia in conferring HF regeneration ability to the DP cells in our system. This direct correlation of hypoxia with perpetuating EMI has not been reported so far in any in vitro HF model systems.

The observed differences in the cell number in the outer zone compared with the inner zone throughout the culture period indicated an increase in cell proliferation in the outer zone. In agreement with this, our histology results showed enhanced ECM production along with closely interacting cells within the DPS + KS-SG organoids. Interestingly, these cells also showed migratory characteristics and were observed to interact and remodel the surrounding SG matrix. Since cell migration and self-assembly through ECMs is fundamental to morphogenetic processes in tissue development, homeostasis, and regeneration (Chameettachal et al., 2016), our findings provide strong evidence that SG per se may contribute toward enhanced DP morphogenesis and thus enhanced HF regenerative property. Overall, our results clearly demonstrated that encapsulating the DPS with supporting cells laden in the SG matrix helped in establishing the HF organoid model (DPS + KS-SG) compared with DPS model, which could recapitulate the expression of at least some of the HF-specific genes and activation of signaling pathways involved in human HF regeneration.

Taken together, this human cell–based model offers unprecedented insights into the role of involvement of (a) DP cells with other cell types, such as HF keratinocytes and HF stem cells, and (b) the SG microenvironment in conferring HF regeneration properties to DPS compared with other existing in vitro models, which mostly consist of murine cells in collagen gels (Kageyama et al., 2018) or irregular-shaped aggregates of limited dimension (Lin et al., 2016). The temporal expression of signaling pathway–specific gene expression of BMPs and β-catenin is indicative of replication of in vivo like HF anagen stage DP cell characteristics. The addition of minoxidil further validated the efficacy of our relatively simpler DPS model in maintaining the anagen hair growth stage. Moreover, it also helped to shed some light on the downstream action of minoxidil on important regulatory signaling pathways as evidenced by the temporal control of BMP signaling by the expression of NOG and the activation of canonical Wnt–β-catenin signaling. In future, it would be interesting to investigate whether the usage of HF keratinocyte and HF stem cells encapsulated in SG can maintain and support the DP's innate ability to induce hair after long-term culture, possibly by preventing differentiation. In addition, further experiments are required to determine how modulation of stiffness of a SG hydrogel can lead to cellular mechanotransduction and spatiotemporal regulation of molecular mechanisms and whether the direct contact of keratinocyte and mesenchymal stem cells in a SG matrix can modulate self-assembly of DP cells, which can be a more efficient strategy for futuristic "HF engineering" protocols. Follow-up studies on minoxidil-treated SG-encapsulated DP organoids will provide better insights into HF biology. Further studies are warranted to validate the organoid model through transplantation in nude mice in terms of induction of HF regeneration.

5 | CONCLUSION

Our study underlines that the in vitro DP organoid model could govern specific gene expression patterns of potentially high relevance to human HF biology. 3D architecture of DP cells, either due to the homotypic or heterotypic cell–cell adhesion or specific microenvironmental features offered by the SG hydrogel, with a putative contribution of hypoxia, could enhance cellular proliferation and matrix synthesis as well as lead to BMP inhibitory signals, and simultaneously upregulation of β-catenin gene expression, a feature that has been extensively found in vivo for enhanced induction of HF regeneration and DP-specific ECM expression. This multicellular organoid model also highlighted the importance of complex epithelial–mesenchymal crosstalks in the activation of HF-specific signaling pathways.

ACKNOWLEDGMENTS

Funding support from ITC Ltd. is acknowledged.

CONFLICTS OF INTEREST

The authors do not have conflicts of interest to declare.

ORCID

Sourabh Ghosh http://orcid.org/0000-0002-1091-9614

REFERENCES

Blanpain, C., & Fuchs, E. (2009). Epidermal homeostasis: A balancing act of stem cells in the skin. *Nature Reviews Molecular Cell Biology*, *10*, 207–217. https://doi.org/10.1038/nrm2636.

Botchkarev, V. A., Botchkareva, N. V., Roth, W., Nakamura, M., Chen, L. H., Herzog, W., … Paus, R., (1999). Noggin is a mesenchymally derived stimulator of hair-follicle induction. *Nature Cell Biology*, *1*(3), 158–64.

Botchkarev, V. A., & Kishimoto, J. (2003). Molecular control of epithelial–mesenchymal interactions during hair follicle cycling. *Journal of Investigative Dermatology Symposium Proceedings*, *8*, 46–55. https://doi.org/10.1046/j.1523-1747.2003.12171.x.

Botchkarev, V. A., Botchkareva, N. V., Sharov, A. A., Funa, K., Huber, O., & Gilchrest, B. A. (2002). Modulation of BMP signaling by noggin is required for induction of the secondary (nontylotrich) hair follicles. *Journal of Investigative Dermatology*, *118*(1), 3–10. https://doi.org/10.1046/j.1523-1747.2002.01645.x.

Chameettachal, S., Midha, S., & Ghosh, S. (2016). Regulation of chondrogenesis and hypertrophy in silk fibroin–gelatin-based 3D bioprinted constructs. *ACS Biomaterials Science and Engineering*, *2*(9), 1450–1463. https://doi.org/10.1021/acsbiomaterials.6b00152.

Chameettachal, S., Murab, S., Vaid, R., Midha, S., & Ghosh, S. (2015). Effect of visco-elastic silk-chitosan microcomposite scaffolds on matrix deposition and biomechanical functionality for cartilage tissue engineering. *Journal of Tissue Engineering and Regenerative Medicine*, *11*, 1212–1229. https://doi.org/10.1002/term.2024.

Chan, C.-C., Fan, S. M. Y., Wang, W. H., Mu, Y. F., & Lin, S. J. (2015). A two-stepped culture method for efficient production of trichogenic keratinocytes. *Tissue Engineering Part C: Methods*, *21*(10), 1070–1079. https://doi.org/10.1089/ten.tec.2015.0033.

Chawla, S., Chameettachal, S., & Ghosh, S. (2015). Probing the role of scaffold dimensionality and media composition on matrix production and phenotype of fibroblasts. *Materials Science and Engineering C*, *49*, 588–596. https://doi.org/ 10.1016/j.msec. 2015.01.059.

Chawla, S., & Ghosh, S. (2017). Establishment of in vitro model of corneal scar pathophysiology. *Journal of Cellular Physiology*, *233*, 3817–3830. https://doi.org/10.1002/jcp.26071.

Chawla, S., & Ghosh, S. (2018). Regulation of fibrotic changes by the synergistic effects of cytokines, dimensionality and matrix: towards the development of an in vitro human dermal hypertrophic scar model. *Acta Biomaterialia*, *69*, 131–145. https://doi.org/10.1016/j.healthpol.2016.12.009.

Chawla, S., Kumar, A., Admane, P., Bandyopadhyay, A., & Ghosh, S. (2017). Elucidating role of silk–gelatin bioink to recapitulate articular cartilage differentiation in 3D bioprinted constructs. *Bioprinting*, *7*, 1–13. https://doi.org/10.1016/j.bprint.2017.05.001.

Chawla, S., Midha, S., Sharma, A., & Ghosh, S. (2018). Silk-based bioinks for 3D bioprinting. *Advanced Healthcare Materials*, *1701204*, 1701204. https://doi.org/10.1002/adhm.201701204.

Chen, D., Jarrell, A., Guo, C., Lang, R., & Atit, R. (2012). Dermal-catenin activity in response to epidermal Wnt ligands is required for fibroblast proliferation and hair follicle initiation. *Development*, *139*(8), 1522–1533. https://doi.org/10.1242/dev.076463.

Das, S., Pati, F., Choi, Y. J., Rijal, G., Shim, J. H., Kim, S. W., … Ghosh, S. (2015). Bioprintable, cell-laden silk fibroin-gelatin hydrogel supporting multilineage differentiation of stem cells for fabrication of three-dimensional tissue constructs. *Acta Biomaterialia*, *11*(1), 233–246. https://doi.org/10.1016/j.actbio.2014.09.023.

Davies, G. C., Julie Thornton, M., Jenner, T. J., Chen, Y. J., Hansen, J. B., Carr, R. D., & Randall, V. A. (2005). Novel and established potassium channel openers stimulate hair growth in vitro: Implications for their modes of action in hair follicles. *Journal of Investigative Dermatology*, *124*(4), 686–694. https://doi.org/10.1111/j.0022-202X.2005.23643.x.

Driskell, R. R., Clavel, C., Rendl, M., & Watt, F. M. (2011). Hair follicle dermal papilla cells at a glance. *Journal of Cell Science*, *124*(8), 1179–1182. https://doi.org/10.1242/jcs.082446.

Dubey, P., Murab, S., Karmakar, S., Chowdhury, P. K., & Ghosh, S. (2015). Modulation of self-assembly process of fibroin: An insight for regulating the conformation of silk biomaterials. *Biomacromolecules*, *16*(12), 3936–3944. https://doi.org/10.1021/acs.biomac.5b01258.

Ehama, R., Ishimatsu-Tsuji, Y., Iriyama, S., Ideta, R., Soma, T., Yano, K., … Kishimoto, J. (2007). Hair follicle regeneration using grafted rodent and human cells. *The Journal of Investigative Dermatology*, *127*(9), 2106–2115. https://doi.org/10.1038/sj.jid.5700823.

Enshell-Seijffers, D., Lindon, C., Kashiwagi, M., & Morgan, B. A. (2010). β-Catenin activity in the dermal papilla regulates morphogenesis and regeneration of hair. *Developmental Cell*, *18*(4), 633–642. https://doi.org/10.1016/j.devcel.2010.01.016.

Epstein, F. H., Paus, R., & Cotsarelis, G. (1999). The biology of hair follicles. *New England Journal of Medicine*, *341*(7), 491–497. https://doi.org/10.1056/NEJM199908123410706.

Fujie, T., Katoh, S., Oura, H., Urano, Y., & Arase, S. (2001). The chemotactic effect of a dermal papilla cell-derived factor on outer root sheath cells. *Journal of Dermatological Science*, *25*(3), 206–212. https://doi.org/10.1016/S0923-1811(00)00130-4.

Furumura, M., & Ishikawa, H. (1996). Actin bundles in human hair follicles as revealed by confocal laser microscopy. *Cell and Tissue Research*, *283*(3), 425–434. https://doi.org/10.1007/s004410050553.

Ghosh, S., Spagnoli, G. C., Martin, I., Ploegert, S., Demougin, P., Heberer, M., & Reschner, A. (2005). Three-dimensional culture of melanoma cells profoundly affects gene expression profile: A high density oligonucleotide array study. *Journal of Cellular Physiology*, *204*(2), 522–531. https://doi.org/10.1002/jcp.20320.

Glotzer, D. J., Zelzer, E., & Olsen, B. R. (2008). Impaired skin and hair follicle development in Runx2 deficient mice. *Developmental Biology*, *315*(2), 459–473. https://doi.org/10.1016/j.ydbio.2008.01.005.

Han, J. H., Kwon, O. S., Chung, J. H., Cho, K. H., Eun, H. C., & Kim, K. H. (2004). Effect of minoxidil on proliferation and apoptosis in dermal papilla cells of human hair follicle. *Journal of Dermatological Science*, *34*(2), 91–98. https://doi.org/10.1016/j.jdermsci.2004.01.002.

Harel, S., Higgins, C. A., Cerise, J. E., Dai, Z., Chen, J. C., Clynes, R., & Christiano, A. M. (2015). Pharmacologic inhibition of JAK-STAT signaling promotes hair growth. *Science Advances*, *1*(9), e1500973–e1500973. https://doi.org/10.1126/sciadv.1500973.

Havlickova, B., Biro, T., Mescalchin, A., Arenberger, P., & Paus, R. (2004). Towards optimization of an organotypic assay system that imitates human hair follicle-like epithelial–mesenchymal interactions. *British Journal of Dermatology*, *151*(4), 753–765. https://doi.org/10.1111/j.1365-2133.2004.06184.x.

Headington, J. T. (1987). Hair follicle biology and topical minoxidil: Possible mechanisms of action. *Dermatology*, *175*, 19–22. https://doi.org/10.1159/000248894.

Higgins, C. A., Chen, J. C., Cerise, J. E., Jahoda, C. A. B., & Christiano, A. M. (2013). Microenvironmental reprogramming by three-dimensional culture enables dermal papilla cells to induce de novo human hair-follicle growth. *Proceedings of the National Academy of Sciences*, *110*(49), 19679–19688. https://doi.org/10.1073/pnas.1309970110.

Hsu, Y. C., Pasolli, H. A., & Fuchs, E. (2011). Dynamics between stem cells, niche, and progeny in the hair follicle. *Cell*, *144*(1), 92–105. https://doi.org/10.1016/j.cell.2010.11.049.

Huang, D., Chang, T. R., Aggarwal, A., Lee, R. C., & Ehrlich, H. P. (1993). Mechanisms and dynamics of mechanical strengthening in ligament-equivalent fibroblast-populated collagen matrices. *Annals of Biomedical Engineering*, *21*(3), 289–305. https://doi.org/10.1007/BF02368184.

Iida, M., Ihara, S., & Matsuzaki, T. (2007). Hair cycle-dependent changes of alkaline phosphatase activity in the mesenchyme and epithelium in mouse vibrissal follicles. *Development Growth and Differentiation*, *49*(3), 185–195. https://doi.org/10.1111/j.1440-169X.2007.00907.x.

Inamatsu, M., Matsuzaki, T., Iwanari, H., & Yoshizato, K. (1998). Establishment of rat derreal papilla cell lines that sustain the potency to induce hair follicles from afollicular skin. *Journal of Investigative Dermatology*, *111*(5), 767–775. https://doi.org/10.1046/j.1523-1747.1998.00382.x.

Irwig, M. S. (2012). Depressive symptoms and suicidal thoughts among former users of finasteride with persistent sexual side effects. *Journal of Clinical Psychiatry*, *73*(9), 1220–1223. https://doi.org/10.4088/JCP.12m07887.

Jahoda, C. A. B., & Christiano, A. M. (2011). Niche crosstalk: Intercellular signals at the hair follicle. *Cell*, *146*, 678–681. https://doi.org/10.1016/j.cell.2011.08.020.

Jahoda, C. A. B., Horne, K. A., & Oliver, R. F. (1984). Induction of hair growth by implantation of cultured dermal papilla cells. *Nature*, *311*(5986), 560–562. https://doi.org/10.1038/311560a0.

Jun-Bo, T., Zhuang-Qun, Y., Xi-Jing, H., Ying, X., Yong, S., Zhe, X., & Tao, C. (2007). Effect of ethosomal minoxidil on dermal delivery and hair cycle of C57BL/6 mice. *Journal of Dermatological Science*, *45*, 135–137. https://doi.org/10.1016/j.jdermsci.2006.09.007.

Kageyama, T., Yoshimura, C., Myasnikova, D., Kataoka, K., Nittami, T., Maruo, S., & Fukuda, J. (2018). Spontaneous hair follicle germ (HFG) formation in vitro, enabling the large-scale production of HFGs for

regenerative medicine. *Biomaterials*, *154*, 291–300. https://doi.org/10.1016/j.biomaterials.2017.10.056.

Kamimura, J., Lee, D., Baden, H. P., Brissette, J., & Paolo Dotto, G. (1997). Primary mouse keratinocyte cultures contain hair follicle progenitor cells with multiple differentiation potential. *Journal of Investigative Dermatology*, *109*(4), 534–540. https://doi.org/10.1111/1523-1747.ep12336704.

Kishimoto, J., Burgeson, R. E., & Morgan, B. A. (2000). Wnt signaling maintains the hair-inducing activity of the dermal papilla. *Genes and Development*, *14*(10), 1181–1185. https://doi.org/10.1101/gad.1410.1181.

Kwack, M. H., Kang, B. M., Kim, M. K., Kim, J. C., & Sung, Y. K. (2011). Minoxidil activates β-catenin pathway in human dermal papilla cells: A possible explanation for its anagen prolongation effect. *Journal of Dermatological Science*, *62*(3), 154–159. https://doi.org/10.1016/j.jdermsci.2011.01.013.

Lachgar, S., Charveron, Gall, & Bonafe (1998). Minoxidil upregulates the expression of vascular endothelial growth factor in human hair dermal papilla cells. *The British Journal of Dermatology*, *138*(3), 407–411. https://doi.org/10.1046/j.1365-2133.1998.02115.x.

Lee, S. H., Lee, Y. J., & Han, H. J. (2011). Role of hypoxia-induced fibronectin-integrin β1 expression in embryonic stem cell proliferation and migration: Involvement of PI3K/Akt and FAK. *Journal of Cellular Physiology*, *226*(2), 484–493. https://doi.org/10.1002/jcp.22358.

Lee, S. H., Yoon, J., Shin, S. H., Zahoor, M., Kim, H. J., Park, P. J., … Choi, K. Y. (2012). Valproic acid induces hair regeneration in murine model and activates alkaline phosphatase activity in human dermal papilla cells. *PLoS One*, *7*(4), e34152. https://doi.org/10.1371/journal.pone.0034152.

Limat, A., Hunziker, T., Waelti, E. R., Inaebnit, S. P., Wiesmann, U., & Braathen, L. R. (1993). Soluble factors from human hair papilla cells and dermal fibroblasts dramatically increase the clonal growth of outer root sheath cells. *Archives of Dermatological Research*, *285*(4), 205–210. https://doi.org/10.1007/BF00372010.

Lin, B., Miao, Y., Wang, J., Fan, Z., Du, L., Su, Y., … Xing, M. (2016). Surface tension guided hanging-drop: Producing controllable 3D spheroid of high-passaged human dermal papilla cells and forming inductive microtissues for hair-follicle regeneration. *ACS Applied Materials and Interfaces*, *8*(9), 5906–5916. https://doi.org/10.1021/acsami.6b00202.

Maretto, S., Cordenonsi, M., Dupont, S., Braghetta, P., Broccoli, V., Hassan, A. B., … Piccolo, S. (2003). Mapping Wnt/beta-catenin signaling during mouse development and in colorectal tumors. *Proceedings of the National Academy of Sciences of the United States of America*, *100*(6), 3299–3304. https://doi.org/10.1073/pnas.0434590100.

Messenger, A. G., Elliott, K., Westgate, G. E., & Gibson, W. T. (1991). Distribution of extracellular matrix molecules in human hair follicles. *Annals of the New York Academy of Sciences*, *642*(1), 253–262. https://doi.org/10.1111/j.1749-6632.1991.tb24392.x.

Misago, N., Toda, Sugihara, Kohda, & Narisawa (1998). Proliferation and differentiation of organoid hair follicle cells co-cultured with fat cells in collagen gel matrix culture. *The British Journal of Dermatology*, *139*(1), 40–48. Available at. http://www.ncbi.nlm.nih.gov/pubmed/9764147.

Mori, O., & Uno, H. (1990). The effect of topical minoxidil on hair follicular cycles of rats. *Journal of Dermatology*, *17*(5), 276–281. https://doi.org/10.1111/j.1346-8138.1990.tb01641.x.

Müller-Röver, S., Foitzik, K., Paus, R., Handjiski, B., van der Veen, C., Eichmüller, S., … Stenn, K. S. (2001). A comprehensive guide for the accurate classification of murine hair follicles in distinct hair cycle stages. *Journal of Investigative Dermatology*, *117*, 3–15. https://doi.org/10.1046/j.0022-202X.2001.01377.x.

Murab, S., Chameettachal, S., Bhattacharjee, M., Das, S., Kaplan, D. L., & Ghosh, S. (2013). Matrix-embedded cytokines to simulate osteoarthritis-like cartilage microenvironments. *Tissue Engineering. Part A*, *19*(15–16), 1733–1753. https://doi.org/10.1089/ten.TEA.2012.0385.

Ohyama, M., et al. (2006). Characterization and isolation of stem cell-enriched human hair follicle bulge cells. *Journal of Clinical Investigation*, *116*(1), 249–260. https://doi.org/10.1172/JCI26043.

Oliver, R. F. (1967). The experimental induction of whisker growth in the hooded rat by implantation of dermal papillae. *Journal of Embryology and Experimental Morphology*, *18*(August), 43–51.

Oliver, R. F. (1970). The induction of hair follicle formation in the adult hooded rat by vibrissa dermal papillae. *Journal of Embryology and Experimental Morphology*, *23*(1), 219–236. 219 LP-236. Available at. http://dev.biologists.org/content/23/1/219.abstract.

Park, B.-S., Kim, W. S., Choi, J. S., Kim, H. K., Won, J. H., Ohkubo, F., & Fukuoka, H. (2010). Hair growth stimulated by conditioned medium of adipose-derived stem cells is enhanced by hypoxia: Evidence of increased growth factor secretion. *Biomedical Research*, *31*(1), 27–34. https://doi.org/10.2220/biomedres.31.27.

Plikus, M. V., Widelitz, R. B., Maxson, R., & Chuong, C. (2009). Analyses of regenerative wave patterns in adult hair follicle populations reveal macro-environmental regulation of stem cell activity. *The International Journal of Developmental Biology*, *53*(5–6), 857–868. doi: 10.1387/ijdb.072564mp.

Rendl, M., Polak, L., & Fuchs, E. (2008). BMP signaling in dermal papilla cells is required for their hair follicle-inductive properties. *Genes and Development*, *22*(4), 543–557. https://doi.org/10.1101/gad.1614408.

Rosenberger, C., Solovan, C., Rosenberger, A. D., Jinping, L., Treudler, R., Frei, U., … Brown, L. F. (2007). Upregulation of hypoxia-inducible factors in normal and psoriatic skin. *Journal of Investigative Dermatology*, *127*(10), 2445–2452. https://doi.org/10.1038/sj.jid.5700874.

Rossi, A., et al. (2012). Minoxidil use in dermatology, side effects and recent patents. *Recent Patents on Inflammation & Allergy Drug Discovery*, *6*(2), 130–136. https://doi.org/10.2174/187221312800166859.

Rufaut, N. W., Nixon, A. J., Goldthorpe, N. T., Wallace, O. A. M., Pearson, A. J., & Sinclair, R. D. (2013). An in vitro model for the morphogenesis of hair follicle dermal papillae. *Journal of Investigative Dermatology*, *133*, 2085–2088. https://doi.org/10.1038/jid.2013.132.

Solanas, G., & Benitah, S. A. (2013). Regenerating the skin: A task for the heterogeneous stem cell pool and surrounding niche. *Nature Reviews Molecular Cell Biology*, *14*, 737–748. https://doi.org/10.1038/nrm3675.

Soma, T., Fujiwara, S., Shirakata, Y., Hashimoto, K., & Kishimoto, J. (2012). Hair-inducing ability of human dermal papilla cells cultured under Wnt/β-catenin signalling activation. *Experimental Dermatology*, *21*, 307–309. https://doi.org/10.1111/j.1600-0625.2012.01458.x.

Soma, T., Tajima, M., & Kishimoto, J. (2005). Hair cycle-specific expression of versican in human hair follicles. *Journal of Dermatological Science*, *39*(3), 147–154. https://doi.org/10.1016/j.jdermsci.2005.03.010.

Tanimura, S., Tadokoro, Y., Inomata, K., Binh, N. T., Nishie, W., Yamazaki, S., … Nishimura, E. K. (2011). Hair follicle stem cells provide a functional niche for melanocyte stem cells. *Cell Stem Cell*, *8*(2), 177–187. https://doi.org/10.1016/j.stem.2010.11.029.

Tiede, S., Kloepper, J. E., Bodò, E., Tiwari, S., Kruse, C., & Paus, R. (2007). Hair follicle stem cells: Walking the maze. *European Journal of Cell Biology*, *86*(7), 355–376. https://doi.org/10.1016/j.ejcb.2007.03.006.

Toyoshima, K., Asakawa, K., Ishibashi, N., Toki, H., Ogawa, M., Hasegawa, T., … Tsuji, T. (2012). Fully functional hair follicle regeneration through the rearrangement of stem cells and their niches. *Nature Communications*, *3*, 3. https://doi.org/10.1038/ncomms1784.

Weinberg, W. C., Goodman, L. V., George, C., Morgan, D. L., Ledbetter, S., Yuspa, S. H., & Lichti, U. (1993). Reconstitution of hair follicle development in vivo: Determination of follicle formation, hair growth, and hair quality by dermal cells. *The Journal of Investigative Dermatology*, *100*(3), 229–236. https://doi.org/10.1111/1523-1747.ep12468971.

Won, C. H., Kwon, O. S., Kang, Y. J., Yoo, H. G., Lee, D. H., Chung, J. H., … Eun, H. C. (2012). Comparative secretome analysis of human follicular dermal papilla cells and fibroblasts using shotgun proteomics. *BMB Reports*, *45*(4), 253–258. https://doi.org/10.5483/BMBRep.2012.45.4.253.

Yen, C. M., Chan, C. C., & Lin, S. J. (2010). High-throughput reconstitution of epithelial–mesenchymal interaction in folliculoid microtissues by biomaterial-facilitated self-assembly of dissociated heterotypic adult

cells. *Biomaterials*, *31*(15), 4341–4352. https://doi.org/10.1016/j.biomaterials.2010.02.014.

Young, T. H., Lee, C. Y., Chiu, H. C., Hsu, C. J., & Lin, S. J. (2008). Self-assembly of dermal papilla cells into inductive spheroidal microtissues on poly(ethylene-co-vinyl alcohol) membranes for hair follicle regeneration. *Biomaterials*, *29*(26), 3521–3530. https://doi.org/10.1016/j.biomaterials.2008.05.013.

How to cite this article: Gupta AC, Chawla S, Hegde A, et al. Establishment of an in vitro organoid model of dermal papilla of human hair follicle. *J Cell Physiol*. 2018;1–16. https://doi.org/10.1002/jcp.26853